Physics-Informed Machine Learning for Structural Health Monitoring of Aerospace Composite Structures

ROHAN CHABUKSWAR, CHLOE MULLEN
and KONSTANTINOS KOURAMAS

ABSTRACT

This paper presents advanced structural health monitoring (SHM) methods for aerospace composite structures, which pose unique challenges due to sensor placement, cost, and environmental exposure. We introduce novel, physics-disciplined, data-driven approaches developed through two European Union projects. The first technique embeds glass-coated copper microwires in carbon-fibre composites, exploiting their Giant Magnetoimpedance (GMI) response to detect, classify, and quantify damage under stress. The second approach supports damage monitoring in composite liquid hydrogen tanks using Fibre Bragg Grating (FBG) sensors, addressing the challenges of conformal geometry and strict leakage tolerance where conventional diagnostics are inadequate. Physics-informed machine learning algorithms are developed for both systems. Finite element simulations inform neural network architecture and feature selection, while simulated signals guide strain and damage modelling. Experimental and simulation-based validation confirms high accuracy in damage detection and characterisation.

This work was funded by the European Union under the Horizon Europe grant 101056884 and by the EU Clean Hydrogen Partnership under Grant Agreement 101101404. Views and opinions expressed are however those of the author(s) only and do not necessarily reflect those of the European Union or Clean Hydrogen Joint Undertaking. Neither the European Union nor the granting authority can be held responsible for them.

1. INTRODUCTION

Unscheduled maintenance and operational disruptions pose significant costs to the aviation industry. In 2015, the 13 largest U.S. airlines incurred USD 5 billion in total costs—USD 2 billion from delays and cancellations, and USD 3 billion from unplanned maintenance [1]. Around 70% of disruptions were due to Line Replaceable Unit (LRU) failures, with 25% of these attributable to predictable factors such as weather, pollution, wear, and malfunction.

Collins Aerospace Ireland, Penrose Wharf Business Centre, Cork, Ireland T23 XN53

Average direct maintenance costs are USD 870 per flight hour, with 40% for engines, and 30% each for airframe and components. Labour accounts for 22% and materials for 60% of these costs [2]. In 2016, the maintenance supply chain held USD 44 billion in inventory—about USD 2.5 million per active aircraft. Warranty reserves totalled USD 2.1 billion for aerospace OEMs and USD 2.3 billion for suppliers [3]. Fault diagnosis and part replacement delays often lead to extended aircraft downtime and further schedule disruptions.

2. PREVIOUS WORK

In the search for optimal algorithms for structural health monitoring (SHM) in composite structures, a comprehensive review of state-of-the-art Artificial Intelligence/Machine Learning (AI/ML) approaches was undertaken. Although previous work on SHM specifically for aerospace composite structures is scarce — and research on composites or aerospace independently is limited — the literature in the broader field of civil engineering (e.g., buildings, bridges, pipelines) offers a substantial basis for survey and analysis.

In the recent literature, state-of-the-art AI/ML approaches have been used for SHM of composite structures. Supervised methods including Decision Trees (DT), Support Vector Machines (SVM), k-Nearest Neighbours and ensemble modelling ([4], [5]) have been used for the classification of damage on structures including composites. The main shortcoming of these methods is the inability to deal with nonlinear corelations between operational parameters and damage features, while their effectiveness and performance drops as the data dimensionality increases.

Neural Network (NN) based approaches have shown to overcome this issue [4]. Deep Learning (DL) methods based on Convolutional Neural Network (CNN) [6], probabilistic NNs [7] and deep autoencoders [8], that have been used for composite SHM algorithms, have the advantage of extracting key features from data and images by using convolutional operations [4], which can be interpreted as mathematical functions operating on data. Any physical restrictions on relationships in the data can be represented as convolutional filters. If these filters are being trained, constraints on these filters in terms of dimensions, sizes, and weight values can be implemented to improve the training and performance while each filter learned in this way can be interpreted as a physical function, and it is possible to compare and adjust the weights using domain knowledge. This gives rise to the so-called physics-disciplined (or physics-inspired) neural networks [6] that we will explore further in this paper.

3. BACKGROUND

SHM refers to the continuous or periodic observation of structural systems through response measurements, enabling the detection of changes in material or geometric properties over time.

3.1 Fibre Bragg Gratings

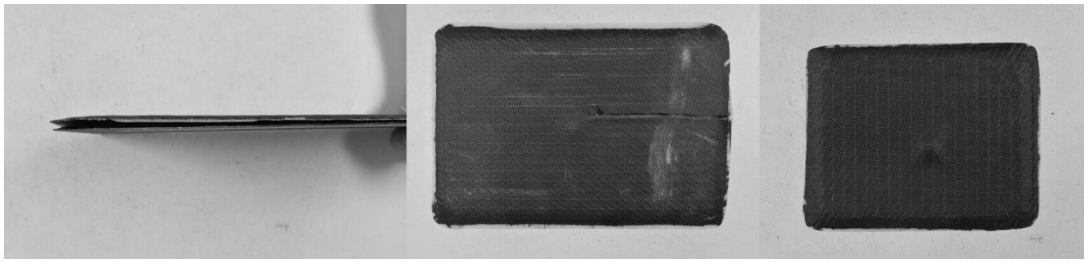

Figure 1: Coupons manufactured by Titania with (a) delamination, (b) crack, and (c) dent damage prior to testing.

Fibre Bragg Gratings (FBGs) are well-suited for detecting localised strain changes caused by damage, as they respond to both average and differential strain along their length. Under uniform strain and temperature, the Bragg wavelength shifts predictably, producing a single, symmetric reflection peak. However, non-uniform strain or temperature gradients—such as those from microcracks—disrupt this coherence, resulting in peak broadening, splitting, or asymmetry. These spectral distortions can be analysed using data-driven methods guided by physical models to detect and characterise damage. Optical sensing is ideal for environments where electrical sensing could present as a hazard, such as the proposed composite liquid hydrogen tank in the COCOLIH_2T project.

3.2 Giant Magnetoimpedance

A key limitation of FBGs is their reliance on continuous connection to data acquisition (DAQ) systems. The associated hardware, including power sources and signal electronics, restricts their embedment within structural components — particularly in aerospace, where mass and volume constraints are critical [9]. The Giant Magnetoimpedance (GMI) effect in glass-coated amorphous microwires offers an alternative, passive sensing modality. These microwires exhibit impedance changes under mechanical stress and can be embedded within composites for contactless strain measurement [10]. Damage-induced strain variations affect their electromagnetic response, enabling detection and localisation using physics-informed AI/ML.

Such sensing modality as proposed in the INFINITE project can benefit aircraft composite components such as fan cowls, thrust reversers, inner inlet barrel, etc. Common damages to these include nicks, scratches, gouges, dents, delamination, disbond, and leading-edge erosion.

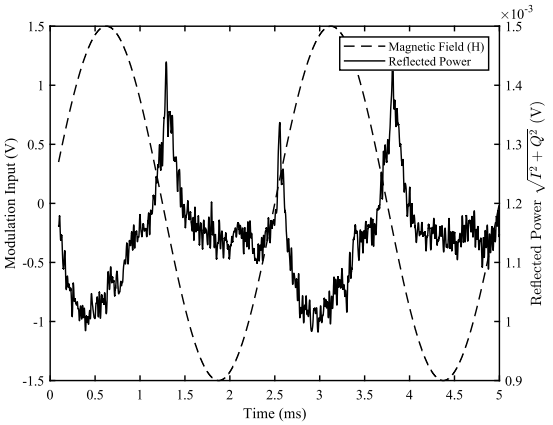

Figure 2: Magnetic field modulation and reflected signal power.

4. APPROACH

Building on these sensing modalities, this work develops physics-informed, data-driven algorithms tailored to each application: FBG-based strain sensing in conformal liquid hydrogen tanks, and GMI-based stress sensing in carbon-fibre composites. Due to practical

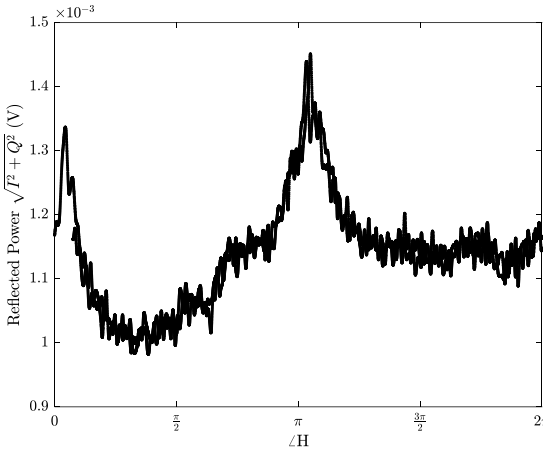

Figure 3: Graph of reflected power vs argument of magnetic field.

limitations in directly modelling the inverse problem, data-driven methods are employed.

4.1 Using Simulation Data

By simulating spectra for a single Bragg wavelength across a range of stress and crack density values, and introducing noise to match experimental conditions, a representative training set is generated. Key features—peak count, position, width (relative to the design wavelength), and height (in dB)—are extracted.

These features are used to estimate strain. Multiple algorithms were down selected and explored, (including linear regression, regression trees, SVMs, Gaussian process regression, and NNs), to estimate the strain using the features from preprocessing, and the best performing one was chosen—in this case, it was an ensemble regression tree. A high-confidence region, which includes only the more physically realistic data, was selected from an algorithm development perspective, however it was guided by limited available data from a cryogenic static test. If the estimated strain falls outside a high-confidence region, crack density is not evaluated as it cannot be reasonably estimated. Within the valid region, crack density is predicted using a second ensemble regression tree down selected from the above list. The results are described in Section 5.1.

4.2 Using Experimental Data

The previous work by the authors [6] detailed the simulation-based down selection and fine-tuning of algorithms for the GMI sensing modality, when delays in manufacturing readers had necessitated the use of simulation data. Once the readers were calibrated and manufactured, data was acquired by using the test setup shown in [11]. Apart from undamaged composite coupons embedded with microwires, coupons manufactured with delamination, dents, or crack damages at different severities were subjected to varying levels of loading stress (from 0 N through 1000 N) while acquiring the data. Figure 1 shows coupons manufactured with delamination, crack, and dent damages by Titania, a consortium partner in the INFINITE project, prior to testing.

TABLE I: MATRIX FOR DAMAGED COUPONS FOR MICROWIRE SENSING TESTS.

Damage	Allowable Limit	Loading Type	Manufactured Damages				
			30%	70%	100%	150%	250%
Delamination (mm)	12.5 mm	Bending	3.75	8.75	12.5	18.75	31.25
Dent (layers)	3 layers	Bending	1	2	3	5	8
Crack (layers)	3 layers	Bending	1	2	3	5	7

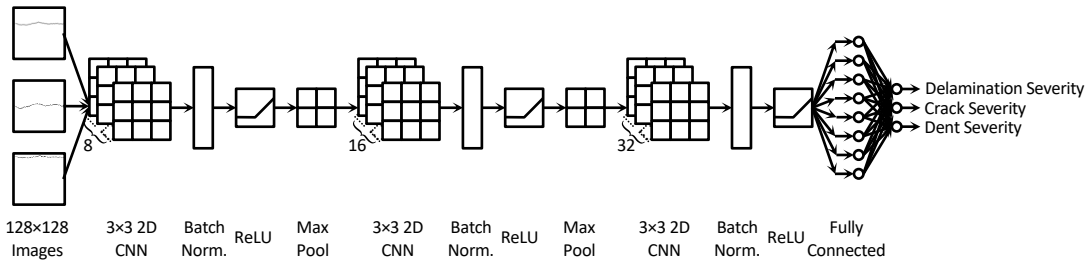

Figure 4: Deep CNN structure for identification and estimation. The final detection and classification of damages is done using thresholding and arg_max.

As shown in TABLE I, the test severities were chosen at 30%, 70%, 100%, 150%, and 250% of the allowable damage limit in aerospace context (assuming an 8-layer coupon). The coupon was subjected to an electromagnetic field modulated at 400 Hz while the transceivers measured the reflection of a 200 kHz electromagnetic signal. This received signal is demodulated and passed through a low pass filter to get the reflection coefficient.

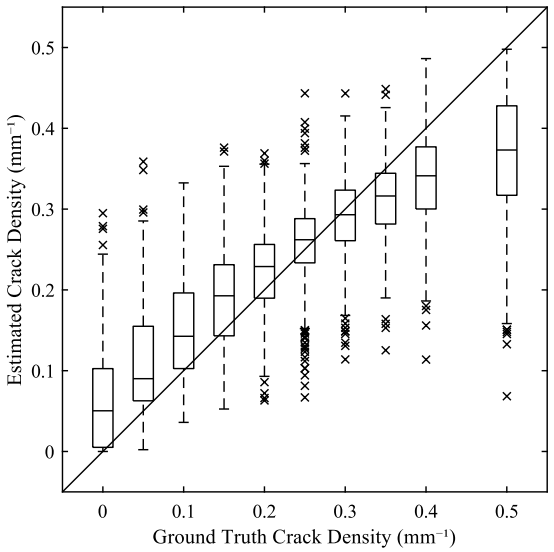

Figure 6: Crack density estimates for the simulation of FBG sensing modality. Severity 0 indicates undamaged samples. Boxes represent the interquartile range with the median line; outliers (>1.5× IQR) are shown as ×.

When this reflection coefficient is plotted against the magnetic field, sharp peaks are observed just after the zero-crossing of the magnetic field, as shown in Figure 2. The width and height of these peaks is dependent on the strain experienced by the microwires, which itself is dependent on the loading stress and the damage. When the reflected power is plotted against the argument of the magnetic field, these peaks overlap as seen in Figure 3. While there can be any number of methods to analyse this data for detection, identification, and estimation of the damage, since this graph itself should be the characteristic of the loading stress and damage, it was first attempted using a deep CNN on 128×128-pixel images of these graphs. The CNN consists of 3 sets of filters, where each set is a convolutional filter followed by max-pooling and a ReLU activation. The final fully connected layer produces three outputs — damage severities for each type — expressed as fractions of the maximum allowable damage. Each output is then compared

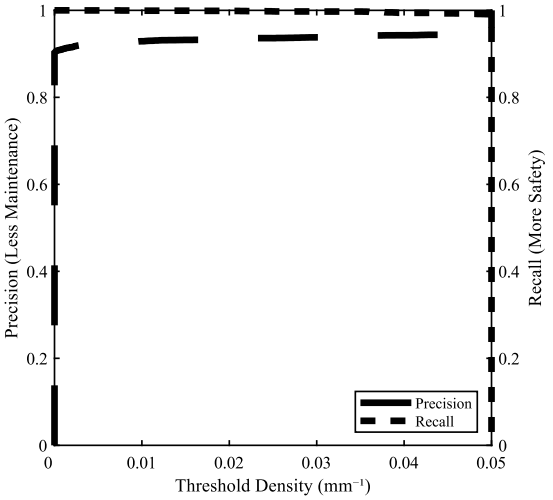

Figure 5: Precision and Recall as a function of threshold crack density for FBG sensing modality.

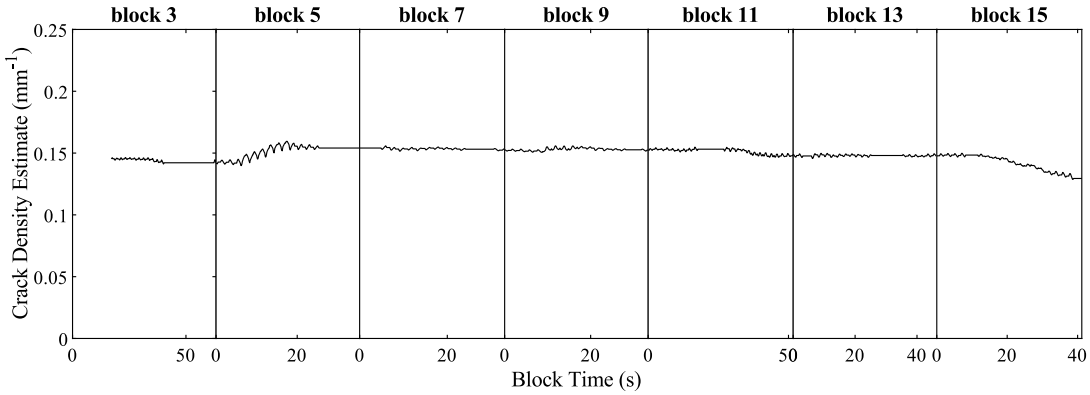

Figure 7: Crack density estimation for experimental data for FBG sensing modality (using a 60-second moving-average).

against a predefined threshold. If all three severities fall below their respective thresholds, the coupon is classified as healthy. If one or more exceed the thresholds, the damage type corresponding to the highest estimated severity is selected as the classification, and that severity value is reported as the estimate. For the classification of damages, the images of data from all the coupons as per the test matrix in TABLE I under all the varying stresses were analysed using a classification deep CNN with the structure shown in Figure 4.

This approach enables unified learning—rather than training separate models for damage type and severity, a single model jointly learns both tasks. Since damage type and severity are intrinsically linked, this shared learning improves efficiency and may enhance generalisation. For non-linear strain responses, combining detection, identification, and estimation allows the model to capture complex interdependencies. With three distinct outputs, the model remains explainable — each prediction reveals how and why a classification was made. This modular architecture also simplifies deployment, version control, and maintenance, and supports future expansion to new damage types. The results are described in section 5.2.

5. RESULTS & DISCUSSIONS

In both cases the algorithms were tuned by partitioning the available data into training and validation sets. As there were some experiments for the FBG sensing

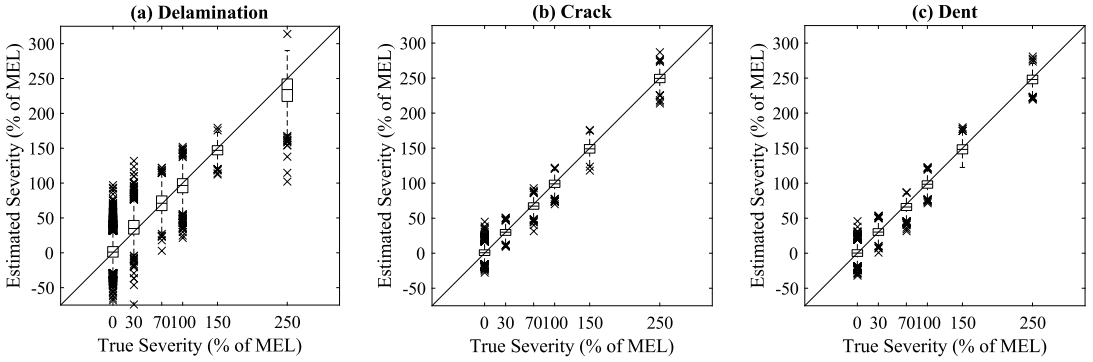

Figure 8: Severity estimates for the testing of microwire sensing modality. Severity 0 indicates undamaged samples. Boxes represent the interquartile range with the median line; outliers (>1.5× IQR) are shown as ×.

modality without any ground truth about crack density, the models tuned on simulation data were tested on experimental data too, to study the robustness of the algorithm and its ability to generalise beyond its training conditions.

5.1 FBG Sensing Modality

Figure 6 shows the prediction of crack density for the simulation data. The correlation coefficient between the estimation and ground truth is 0.8422. For detection, the threshold for crack density was varied between 0 and 0.5 mm^{-1}, and the precision and recall (PR) values as a function of the threshold are shown in Figure 5 for the optimal trade-off between safety and maintenance. The area under the PR curve is 0.9730.

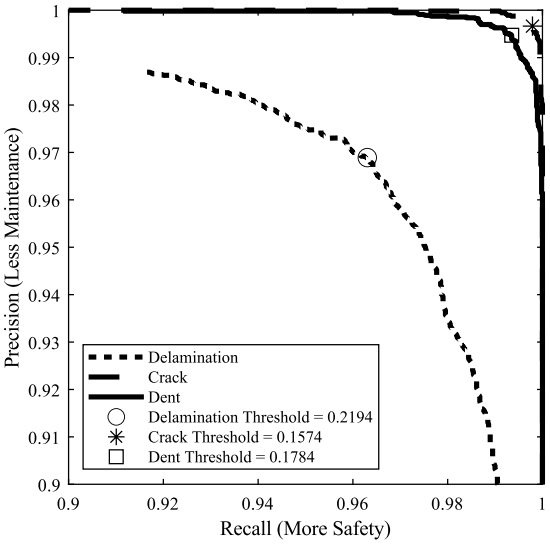

Figure 9: Precision vs. recall curves when threshold severity is varied between 0% and 30% for microwire sensing modality. Note that the lower limits for both the axes are 0.9, not 0, to highlight the difference between the three curves.

Figure 7 shows the estimation of crack density when applied to experimental data. Unfortunately, due to absence of any ground truth, the performance cannot be quantified.

5.2 Microwire Sensing Modality

TABLE II: METRICS & THRESHOLD FOR ESTIMATION OF DAMAGE SEVERITIES.

	Delamination	**Crack**	**Dent**
CC	0.9701	0.9934	0.9933
APR	0.9904	0.99997	0.9998
Threshold	0.2194	0.1574	0.1784

Figure 8 shows the prediction of damage severity for the test data, and TABLE II reports the correlation coefficients (CC) for the same. Figure 9 shows the precision vs. recall curves when threshold severity is varied between 0% and 30%. TABLE II also reports the area under these PR curve (APR), as well as the optimal thresholds chosen, which are also shown in Figure 9. TABLE III shows the confusion matrix between classifications of damages when these optimal thresholds are used.

TABLE III: CONFUSION MATRIX FOR CLASSIFICATIONS OF DAMAGES USING OPTIMAL THRESHOLDS IN TABLE II.

		True Labels			
		Healthy	**Delamination**	**Crack**	**Dent**
Predict.	**Healthy**	93.34%	5.25%	0.55%	0.86%
	Delamination	3.44%	96.16%	0.20%	0.20%
	Crack	0.22%	2.52%	97.17%	0.09%
	Dent	0.66%	1.35%	0.14%	97.85%

6. CONCLUSIONS

The main contributions of the paper are to present a synergy between two distinct but related damage detection and severity estimation applications using physics-disciplined AI/ML. The proposed methodology incorporates safety by design which is vital in aerospace. Both projects demonstrate the benefits of adding physics-based constraints to make a more reliable and generalisable model, with application across both simulation and experimental scenarios, by strategically integrating heterogenous data preprocessing and algorithmic frameworks. This underscores the potential for physics disciplined AI/ML to bridge the gap between theoretical models and practical SHM applications, offering a powerful tool for enhanced structural integrity assessment and informed maintenance decisions in the aerospace context.

REFERENCES

[1] US Bureau of Transportation Statistics, US Dept. of Transportation, "Transportation Statistics Annual Report US DOT Form 41," 2016.

[2] International Air Transport Association (IATA) Maintenance Cost Task Force (MCTF), "Airline Maintenance Cost Executive Commentary—An Exclusive Benchmark Analysis of Maintenance Cost Task Force (MCTF) FY 2013," 2014.

[3] Warranty Week, "Aerospace Warranty Expense Report," 13 April 2017. [Online]. Available: http://www.warrantyweek.com/archive/ww20170413.html.

[4] X. Zhu, Z. Cai, J. Wu, Y. Cheng and Q. Huang, "Convolutional neural network based combustion mode classification for condition monitoring in the supersonic combustor," *Acta Astronautica,* vol. 159, p. 349–357, 2019.

[5] R. K. Langat, W. Deng, E. De Luycker, A. Cantarel and M. Rakotondrabe, "In-situ piezoelectric sensors for structural health monitoring with machine learning integration," *Mechatronics,* vol. 106, p. 103297, 2025.

[6] R. Chabukswar, C. Mullen and K. Kouramas, "On the Training of Algorithms Using Finite-Element Computation Data for Damage Identification in Sensorised Composite Structures," in *9th European Congress on Computational Methods in Applied Sciences and Engineering (ECCOMAS)*, Lisbon, 2024.

[7] S. Na and H.-K. Lee, "Neural network approach for damaged area location prediction of a composite plate using electromechanical impedance technique," *Composites Science and Technology,* vol. 88, p. 62–68, 2013.

[8] M. Rautela, J. Senthilnath, E. Monaco and S. Gopalakrishnan, "Delamination prediction in composite panels using unsupervised-feature learning methods with wavelet-enhanced guided wave representations," *Composite Structures,* vol. 291, no. 115579, 2022.

[9] M. Al Ali, P. Platko, V. Bajzecerova, S. Kusnir, S. Kmet, S. Nalevanko, A. Spegarova, L. Galdun and R. Varga, "Application of bistable glass-coated microwire for monitoring and measuring the deformations of metal structural members," *Measurement,* vol. 208, 2023.

[10] D. Praslicka, J. Blazek, M. Smelko, J. Hudak, A. Cverha, I. Mikita, R. Varga and A. Zhukov, "Possibilities of Measuring Stress and Health Monitoring in Materials Using Contact-Less Sensor Based on Magnetic Microwires," *IEEE Transactions on Magnetics,* vol. 49, no. 1, p. 128–131, 2013.

[11] V. Zhukova, P. Corte-León, J. M. Blanco, A. Allue, M. Ipatov, A. Zhukov and K. Gondra, "Applications of Co-rich Amorphous Glass-coated Microwires for Monitoring the Matrix Polymerization," in *2024 IEEE Applied Sensing Conference (APSCON)*, 2024.